

# Digital data transmission system with capacitive coupling for in-situ temperature sensing in lithium ion cells



Nora Martiny<sup>a,\*</sup>, Thomas Mühlbauer<sup>a</sup>, Sebastian Steinhorst<sup>a</sup>,  
Martin Lukasiewicz<sup>a</sup>, Andreas Jossen<sup>b</sup>

<sup>a</sup> TUM CREATE, 1 CREATE Way, 10-02, CREATE Tower, Singapore 138602, Singapore

<sup>b</sup> Technische Universität München, Lehrstuhl für Elektrische Energiespeichertechnik, Arcisstr. 21, 80333 München, Germany

## ARTICLE INFO

### Article history:

Received 29 July 2015

Received in revised form 2 October 2015

Accepted 2 October 2015

Available online 31 October 2015

### Keywords:

Wireless data transmission

Capacitive coupling

Lithium ion pouch cell

Digital data

Temperature monitoring

In-situ sensing

## ABSTRACT

Precise temperature measurement within a narrow time frame is crucial for the safe operation of Li-Ion battery cells. This paper proposes a digital approach for in-situ cell temperature measurement, relying on capacitive coupled data transmission between the controller in a cell and an external controller. In contrast to purely analog solutions, the digital approach satisfies all requirements in terms of electrochemical, space and transmission quality. For this purpose, analog and digital conceptual hardware setups were implemented for comparison and extensive measurements were carried out. The experimental results for the digital implementation show the influence of capacitor sizes and baud rates, providing a guideline for transmission rates for different sizes of cells. The paper also discusses in detail integration aspects for the digital approach. From the digital concept setup, valuable information is deduced regarding the communication latency, achievable energy consumption and miniaturization potential: Depending on the employed sampling rate, the transmission duration for one message with five temperature values can be reduced to as little as 65  $\mu$ s with a power consumption in the  $\mu$ W range. The proposed miniaturization enables an efficient, low cost, fully integrated logic circuit for data collection and transmission with a size not bigger than 2 mm  $\times$  3 mm.

© 2015 Elsevier Ltd. All rights reserved.

## 1. Introduction

Lithium Ion (Li-Ion) batteries are utilized increasingly in everyday applications from mobile devices over power tools up to electric cars. Compared with other chemistries, the success of Li-Ion batteries has its foundation in the combined high energy and power density as well as high voltage, enhanced lifetime, and the absence of severe memory effects. To ensure the operation within their predefined bounds in terms of voltage and temperature, Li-Ion batteries require sophisticated Battery Management System (BMS). With a well-designed and precise BMS, lifetime of batteries is optimized while safety risks are minimized. As a result, the demand for safe and long-lasting operation strategies is satisfied [1].

One crucial factor when dealing with Li-Ion batteries is the temperature. Higher overall temperatures in the cell mainly lead to an accelerated aging, resulting from a loss of capacity and a rise in internal resistance. On the other hand, an internal cell temperature exceeding the designated range during cycling may be an early indicator for safety-relevant failures. With the emerging trend of

increasing cell sizes, particularly in automotive applications, considerable inhomogeneities within the temperature distribution have to be faced. Arunachala presented in [2] simulation results of cells with different sizes and cooling strategies and showed that temperature gradients can be above 10 K in large-scale automotive cells. To find optimal operating conditions and to detect early failures, permanent, space resolved and reliable temperature monitoring is therefore inevitable.

In most current applications, monitoring is performed by attaching sensors to the surface of battery cells, see [3]. However, this approach has severe drawbacks, particularly in large scale applications where active cooling is applied. In this scenario, battery cells are actively cooled from their surface either using cold air or liquid. The resulting temperature discrepancy between the cell surface and its interior might become significant [2], especially in the event of a thermal runaway [4]. Consequently, the delay in time response when detecting the actual cell temperature may result in an inappropriate battery management when only the surface temperature is monitored. Therefore, an in-situ temperature monitoring as described in [5–7] is of great value.

As mentioned above, space resolved temperature monitoring is necessary in order to observe the State-of-Safety (SoS) at any time, particularly for large cells. However, the collection of a large

\* Corresponding author.

E-mail address: [martiny@tum.de](mailto:martiny@tum.de) (N. Martiny).

amount of sensor data is challenging when applying in-situ sensing, see [5,8,9]. For wire-based data transmission systems, leakage at the sealant becomes a severe issue, resulting in long-term instability of cells. To eliminate these problems, the paper at hand proposes data transfer without additional feed through wiring from multiple sensors in the cell.

In [5,8,9], thin-film thermocouples are implemented as simple and reliable solution. Since these sensors require a reference temperature at the cold junction, they are not suitable for fully integrated solutions. Therefore, resistance based sensors have been applied in [10] to measure the cell temperature at different points and read the data out via capacitive coupling. However, an efficient implementation of the proposed data transfer scheme is prohibited due to the high practical complexity. As a remedy, the paper at hand proposes a fully digitized solution.

**Contributions of the paper.** This paper proposes a fully integrated digital solution for in-situ temperature sensing in Li-Ion cells. As a result, it overcomes all drawbacks of existing data-transmission solutions for in-situ measurements and allows for an efficient integration on a large scale.

In Section 2, related work in the domain of Li-Ion and in-situ temperature sensing is discussed. Particularly, limitations of previous work as well as resulting challenges are pointed out. A more detailed discussion on in-situ temperature sensing is given in Section 3, deducing the requirements for the proposed solution.

The proposed approach for a fully integrated digital solution and the setup of a proof of concept is described in Section 4. This solution has several benefits:

- The delay in time response when detecting the actual cell temperature is reduced to a minimum.
- Space resolved temperature monitoring becomes possible with the used data transmission protocol.
- A fully integrated solution of the described hardware might be produced at very low cost.

It furthermore integrates with the emerging technology of smart cells [1] where the battery management is distributed onto controllers which are directly attached to the batteries.

Section 5 discusses solutions for the integration as well as the potential towards miniaturization of specific components. Performed experiments and their results are elaborated and the robustness of the proposed system is investigated. Furthermore, the energy consumption of the solution is determined and strategies to keep it at minimum are discussed.

Experiments that show the influence of capacitor size and baud rate on the signal quality and the reliability of the data transmission are presented in Section 6.

The paper is finally concluded in Section 7, giving an outlook of resulting challenges and future work.

## 2. Related work

Due to the growing demand for Li-Ion batteries and their safe and reliable operation [11,12], the estimation of the internal temperature of Li-Ion cells is a focus interest of ongoing research. Several papers use internal cell parameters like the impedance spectrum to estimate the temperature, see [13,14]. Other research considers the integration of sensors physically into the cells [5–9,15]. Both methods, however, have their specific drawbacks as outlined in the following.

While using internal parameters has the advantage of being non-invasive and in result non-influential on the cell behavior, so far no possibility has been found to estimate inhomogeneities and temperature hotspots with these methods. This means, that only

an average temperature of the cell can be detected and safety hazards are hardly recognizable.

Placing physical sensors into the cells solves these problems and provides the possibility of monitoring the temperature distribution in a cell more accurately [8,9]. Most of the present projects, however, use thermocouples for temperature measurements [5,6,8,9] that require a reference temperature at the cold junction of the sensor in order to estimate absolute temperature values. A feed through the cell casing is mandatory which can lead to leakage [8–10].

In [7,10,15], resistance based sensors are introduced to overcome the drawbacks of requiring a reference temperature. They provide in principle the possibility of encapsulated temperature measurements in the cell if data transmission can be performed wirelessly.

Otto et al. [16] proposed to move the monitoring and control hardware of the lowest layer of a hierarchical battery management system closer to the cells. It is suggested that sensing elements for temperature, current, voltage, impedance and some other cell parameters along with basic cell balancing systems, data processing and the data communication system are integrated into one macro-cell. The macro-cell consists of four pouch cells, connected in series.

Lorentz et al. [17] suggest, similar to the paper at hand, to use a capacitive data communication for battery cell monitoring. The proposed monitoring system provides one temperature sensor, that, along with other monitoring electronics is attached to the surface of a cell. The capacitive data transmission is used to send data from each cell in a module to the common BMS. By contrast, the novelty in the paper at hand is that the described communication system is designed such that it can monitor multiple in-situ temperature sensors and communicate data wirelessly through the cell casing.

In [10], different methods for data transmission are investigated without any additional wiring, showing that existing transmission systems like wireless networks, RFID or power-line communication are not applicable for Li-Ion cells due to space restrictions or shielding effects of the cell casing. As potential solutions [10], suggests capacitive coupling combined with frequency cross over for reading out data from multiple sensors without additional wiring. For the detection of temperature inhomogeneities in the cell, multiple sensors distributed over the whole area are employed. Analog sine waves with a defined frequency are sent into the cell and with the help of frequency crossover, the discussed resistive temperature sensors are read out individually and simultaneously through the coupling capacitors. Nevertheless, this method has its drawbacks as it is practically not implementable at a reasonable effort and costs as the paper at hand shows in the next section. As a remedy, this paper provides a fully digital approach that overcomes all drawbacks of previous approaches.

## 3. Requirements for in-situ sensing

Previous work [9] lists requirements for the integration of measurement electronics into Li-Ion battery cells. It is elaborated that particularly for laminated Li-Ion pouch cells, the integration of measurement electronics is challenging due to the limited space, the sensitivity of the electro-chemical processes on disturbances and the difficulty in sealing the pouch laminate when wires are fed through. As a countermeasure, [10] suggests a wireless solution for the data transmission which is, however, not practically implementable due to its analog high frequency requirements.

In the following, based on the requirements from [9], design criteria for a fully digitized temperature measurement system with data transmission via capacitive coupling are developed. The overall goal when integrating measurement electronics into a battery cell is to affect the behavior of the cell as little as possible

while providing vital information about internal cell parameters like the temperature throughout the whole battery life. This goal can be reached by considering the following criteria.

**Chemical requirements:** As LiPF<sub>6</sub>-based solutions are widely used as electrolyte in state-of-the-art Li-Ion cells, which react with traces of water to Hydrofluoric Acid (HF), the used components need to withstand this acid to ensure an operation of the system throughout the entire battery life.

**Electrochemical requirements:** The location of the measurement system needs to be chosen such that the ionic flow between the active materials of anode and cathode is not interrupted. Furthermore, materials have to be selected for the devices that are inert in the given environment or provide a sufficient and long lasting coating. As this paper deals mainly with the solution for data communication, this requirement, as well as above mentioned chemical requirements, exceeds the scope of the paper and is not addressed in the following. It remains part of future work.

**Shape requirements:** For most applications, especially in the mobile or automotive sector, space is a limiting factor which leads to the demand of cells with a maximized energy density. Furthermore, irregularities in the distance between two electrodes can lead to an inhomogeneous current density in the electrodes and therefore temperature hotspots or accelerated aging. To avoid this, the integrated electronics have to be as small as possible. Sensors or rather sensor matrices, for space resolved measurements, should ideally be placed between electrodes to measure the temperature where it emerges and to detect hot spots. Considerations for the miniaturization of the concept, described in this paper, are therefore addressed in Section 5.

**Data transmission requirements:** The transmission of data from the sensors inside the cell has to be possible without additional wiring at low cost in a reliable manner. Such a solution that fulfills these requirements is the major contribution of this paper.

To stress the importance of the contribution of the paper at hand, the analog data transmission solution [10] is discussed in the following, pointing out the drawbacks that emerge for its practical implementation. For this purpose, the setup, which has been proposed and validated by simulation in [10], has been implemented as shown in Fig. 1. A sine wave is generated with an AD9850 from Analog Devices and sent through an aluminum laminate sheet via a coupling capacitor. The signal is then separated by a frequency crossover that, with the help of bandpass filters, selects the respective measurement resistor  $R_{meas,i}$ .

For investigating the signal's quality over the different branches of the frequency crossover, voltage measurements between  $X_i$  and  $E$  and between  $D$  and  $E$  according to Fig. 1 have been performed.

The difference  $V_{(X_i-E)} - V_{(D-E)}$  that shows the fraction of the signal that is transmitted over a certain measurement resistor is displayed in Fig. 2. The annotated values in the diagram show the corresponding calculated values for the same setup. It can be seen that for low frequencies, the calculated and measured values are in good accordance while for higher frequencies the measured values are much lower than the calculated values. For the sixth branch, the difference between the calculated value  $f_{calc} = 5.03$  MHz and the measured value is in the range of 2 MHz. This can be probably attributed to parasitic capacitances in the setup.

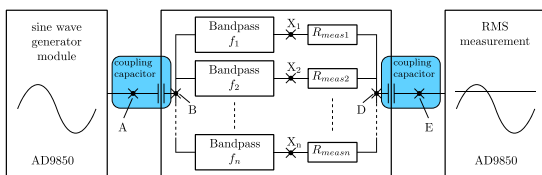


Fig. 1. Setup of the analog system as proposed and simulated in [10] and realized here for suitability studies.

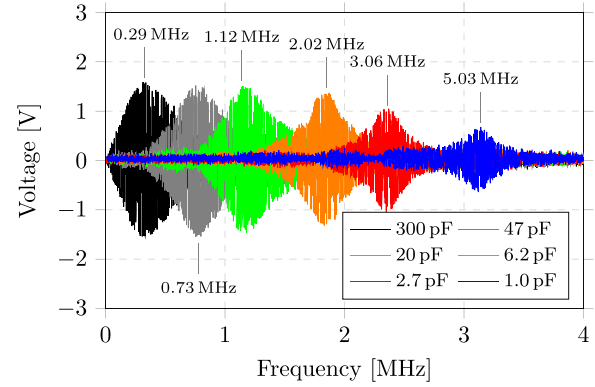


Fig. 2. Measured frequency values over the different measurement resistors – from point  $X_i$  to point  $D$  in 1. The annotated values (in MHz) depict the corresponding calculated values.

Another significant finding when looking into Fig. 2 is the reduced signal strength with higher frequencies while the spread is wider. As a result, for higher frequencies the distinction between the different branches is almost impossible, since the measurement signal of one branch and the noise of the other branches show a similar amplitude. Consequently, for encountering the overlap of signals, the frequency range would need to be extended to even higher frequencies. The given results show clearly that the analog method is therefore not suitable, resulting in the demand for the development of a fully digitized solution.

#### 4. Implementation

Due to the mentioned difficulties in the analog solution for space resolved in-situ measurement, a digital solution that can be integrated into a cell is developed. As proof of concept and to test the communication, a conceptual hardware setup is built with standard components. With this setup, schemes for transmitting the measured data through the pouch cell laminate are investigated. Coupling capacitors as used in the analog solution from [10] are applied for the data transmission through the cell casing.

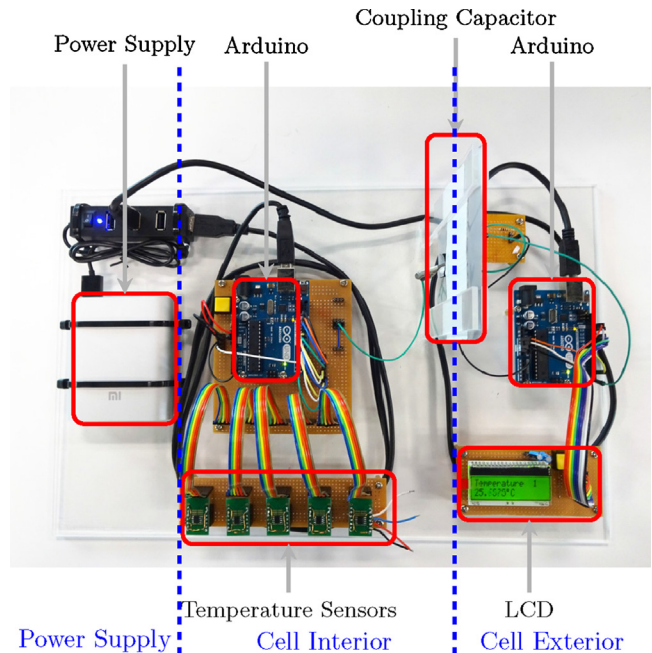


Fig. 3. Conceptual hardware setup for digital data transmission through an aluminum laminate.

#### 4.1. Setup

The hardware setup consists of four parts that are further described in the following and outlined in Fig. 3: the power supply, the cell interior, the coupling capacitor, and the cell exterior.

**Power supply:** The power is supplied by a power bank, based on Li-Ion cells, that provides up to 2.1 A output current and 5.1 V output voltage via a Universal Serial Bus (USB) plug. A USB-hub distributes the power for the interior and exterior part of the setup. In later implementations, this part can be omitted as the required power can be directly obtained from the cell at which the system is integrated.

**Cell interior:** The interior is the part that for the actual implementation shall be integrated into the battery cell. Five integrated temperature sensors ADT7310 from Analog Devices are used to provide distributed temperature data. The temperature sensors are connected via a Serial Peripheral Interface (SPI) interface to an Arduino Uno R3 with an ATmega328P micro controller from Atmel. The Arduino provides all required connectors. A switch for the manual selection of different program modes is added.

**Coupling capacitor:** Between the interior and exterior, a mount for an aluminum laminate sheet is used which represents the battery cell surface. Capacitors of different sizes can be attached to the sheet for investigating sizing effects on the data transmission. On each side of the sheet one capacitor plate made of aluminum foil is glued to the laminate.

**Cell exterior:** A 1 k $\Omega$ -resistor is connected to the exterior capacitor plate which provides two functions: On one hand, it serves as part of a voltage divider – the other part of the divider is integrated in the Arduino – to pull the signal to a desired reference level. On the other hand, this resistor is necessary to create a voltage change over the resistor out of the received current. A second Arduino Uno R3 receives and processes the data and displays the values accordingly on the display on the right lower corner of the setup.

#### 4.2. Data transmission through the coupling capacitor

The data transmission through the coupling capacitors is implemented using the Universal Asynchronous Receiver/Transmitter (UART) standard. This method was chosen as it is a well established data communication protocol that provides a stable data transmission with little likelihood of errors.

One transmitted data set consists of one start byte, two data bytes per temperature sensor and two Cyclic Redundancy Check (CRC) bytes. As in the current setup, five temperature sensors are used, the data set has 13 bytes.

The start byte is chosen such that it is a unique binary sequence that does not correspond to any possible measured temperature value. It is set to 10101010, which corresponds to  $-172^{\circ}\text{C}$  and is outside the temperature range of the applied temperature sensors.

The CRC check sum is calculated individually for each data set by dividing the data bits by a polynomial that is known to both, transmitter and receiver, and comparing the rest. Even small changes in the transmitted data string lead thus to discrepancies in the CRC and provide a simple and reliable error detection.

In case that the start bit sequence of the start byte appears within the normally transmitted temperature values and hence is mistaken to be the start byte, the CRC returns “wrong” and the readout of the received data continues. Only if the start byte and the check sum are correct, the data string is detected as correct and further processed.

With the given setup, a much more stable data transmission than it was described in [10] is realized. This is mainly due to the fact that all data are transmitted digitally and errors are therefore almost omitted.

### 5. Integration

The development platform setup presented in this paper is a proof of concept for the proposed data transmission scheme, using standard components. For integration into a cell, different considerations regarding size adjustments, energy consumption but also the performance of the system have to be made that are addressed in the following.

#### 5.1. Latency of the system

One major reason why in-situ temperature measurement is desired is the faster detection time in case of failures compared to measurements on the cell [9]. Reactions in the worst case situation of a thermal runaway can happen fast and may not be detectable on the cell's surface within a timescale that allows to shut off the cell before serious damage to the surroundings occurs. Feng et al. show in [4] that the stage leading to a thermal runaway where the separator is already melted and micro short circuits start to evolve happens within roughly 50 s with an increasing velocity closer to the separator break up. Being closer to the critical point where the thermal runaway starts makes a high monitoring frequency necessary.

For evaluating the time that one measurement requires with the current implementation, we have conducted an experiment where a button press triggers the system to wake up and start a measurement, which was captured with a scope. The signal curves for a symbol rate of 2,000,000 bd are shown in Fig. 4.

After receiving the data from the sensors ( $\overline{CS}_i$ ), the micro controller requires a short period for calculating the CRC. This phase is between *Start CRC-16* and *Start UART* in Fig. 4. When the CRC calculation is done, the data are sent via the UART interface to the outside.

It is possible to reduce the duration of the SPI communication between sensors and controller ( $\overline{CS}_i$ ). The minimum clock duration can be calculated to 210 ns by adding the different minimum time parameters of the SPI communication, which are given in the data sheet of the ADT7310 [18]. The used default clock speed is set to 4 MHz in the library for the serial communication of the Arduino. This corresponds to a duration of 250 ns. As this influences the latency only marginally but makes the communication more error-prone, it is recommended not to change the clock speed.

In Fig. 4 it can be seen that the calculation of the CRC-16 check sum requires 55  $\mu\text{s}$ . However, the CRC-16 calculation could also be done in hardware. Since using a hardware module needs just 1 cycle per bit, the CRC-16 calculation time could be reduced to 6.875  $\mu\text{s}$  for a 16 MHz controller. Further time saving can be achieved by performing the CRC-16 calculation during the transmission of the first values.

Different to the CRC-16 computation where the latency can be decreased by changing the system structure, the time for UART communication can be influenced by simply increasing the baud rate for the serial communication.

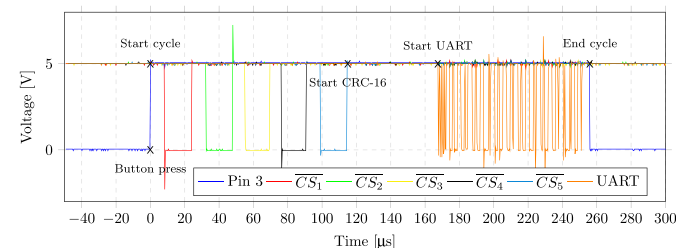


Fig. 4. Latency of the measurement and communication at 2,000,000 bd.



**Table 1**

Duration for the transfer of one bit at different baud rates and transmission time for a temperature measurement message containing 5 temperature values resulting in 130 bit in total.

Baud rate [bd]	Duration per bit	Duration for message
9600	104 $\mu$ s	13.52 ms
750,000	1.33 $\mu$ s	172.9 $\mu$ s
2,000,000	500.0 ns	65 $\mu$ s

Table 1 shows the duration of the UART block from Fig. 4 for a single bit and a complete temperature message for different transmission rates.

With the above calculations, a total time for one measurement of 250  $\mu$ s is estimated for the presented setup. Consequently, with 2,000,000 bd, up to 4000 measurements per second can be made. Depending on the current temperature and the load, the BMS has to decide how often it acquires the temperature values.

### 5.2. Energy consumption

To estimate the energy consumption of the system, two different states have to be considered: the idle state and the active state.

The idle state is the state when the cell is not in use and thus the battery management system is inactive. During this time the system consumes practically no energy and only contributes with very small leak currents of the power supply module presumably in the  $\mu$ A-range to the self-discharge of the cell.

The active state is the state when the system is powered up, conducting a measurement and sending the values to the outside. During this time, the system has to be supplied by the power module. The energy consumption is thereby proportional to the sampling rate. The described hardware setup is powered with 5 V and not yet optimized for low power applications in the battery voltage range of 2.7–4.2 V. It is therefore assumed that in a later application using a dedicated low-power System-on-Chip implementation, the energy consumption will be orders of magnitude lower than the currently consumed 100 mW under full load.

### 5.3. Miniaturization

As mentioned above, the presented hardware setup consists of standard components to test the data communication principle. For an integration into a cell, the system needs to be miniaturized. In the following, we will discuss which parts of the hardware setup are necessary for a future system. In a next step, a solution for the miniaturization of the required components is proposed.

Fig. 5 shows the modules that need to be integrated into the cell. The external control unit starts the system by sending an enable signal to the integrated DC/DC converter through the coupling capacitor. The DC/DC converter then starts supplying the system. Whether a DC/DC converter is actually required is determined by the Application-Specific Integrated Circuit (ASIC) implementation used for the computational part of the system. The sensors 1 to 5 start measuring and the control unit reads out every sensor once. As soon as it has received the value of each sensor, it sends the data together with the calculated CRC-16 check sum through the coupling capacitor to the external control unit. After all data is sent, the internal control unit powers itself down by switching the DC/DC converter in the sleep mode for saving energy. As the external control unit is integrated in a BMS that already performs voltage sensing, access to the battery terminals is given and hence they can be used as reference points for the power supply.

The coupling capacitor is not further mentioned in this part since it is realized through a thin aluminum foil layer fixed to the

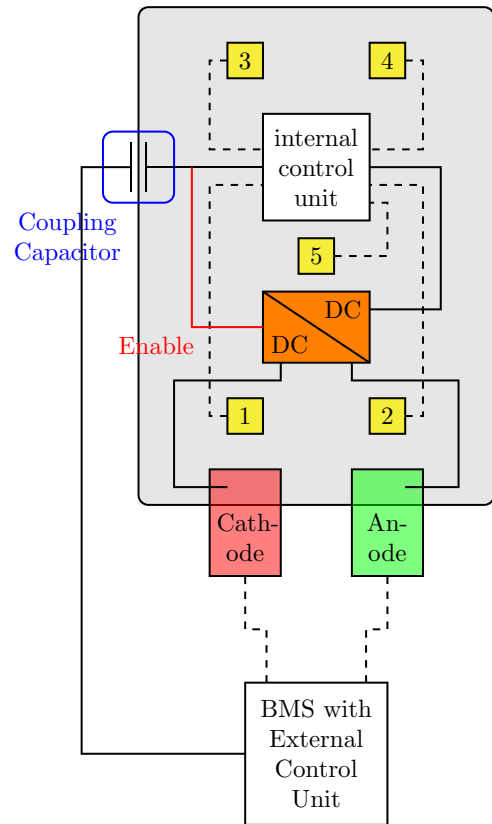


**Fig. 5.** System setup as it can be integrated in one cell with five temperature sensors (1–5) and power supply directly from the cell.

pouch cell laminate and thus it does not contribute to the integrated circuits which have to be minimized in size.

**Frequency generation.** As part of the control unit, a frequency generation unit is necessary. Most of the established micro controllers have an integrated clock generation module. This is however strongly dependent on the temperature, while a crystal shows just very small dependencies on the temperature. Since the temperature inside the cell varies strongly during the operation of the system, a temperature independent clock generation unit is necessary. Thus for the considered system, a crystal oscillator is suggested. The size of this component varies depending on its frequency and is usually in the range of a few mm<sup>2</sup>.

**Controller.** While the micro controller *ATmega168A* used in the development platform is already very small, most of its functions are unused in this application. For the development of a specific ASIC as a System-on-Chip (SoC), it is necessary to know the actual tasks of the control unit. Three main tasks have to be performed: acquiring the data from the sensors, calculation of the CRC-16 check sum and the transmission of data through the asynchronous serial interface.

For acquiring the data from the sensors, a certain request sequence has to be sent as shown in Section 4. This is a fixed process which can be implemented as a static logic circuit. The calculation of the CRC-16 was discussed in Section 4 and it was shown that this calculation is even faster if it is made by a hardware realization with a simple shift register and XOR gates.

Finally, the data has to be transmitted to the external control unit over the serial interface. Therefore, a clock signal is necessary on whose edges the bits are shifted out. There are no computational costs for this process which can be performed with appropriate logic. Thus, the control unit to be designed does not necessarily require a processor and could be realized with fixed

logic gates, mostly representing shift registers. Consequently, the logic circuitry comprising less than 10,000 transistors can be implemented as a very efficient and cheap ASIC. The footprint of such an ASIC could be in the range of a 2 mm × 3 mm 6-lead plastic Dual-Flat No-leads (DFN) package with a power consumption in the  $\mu\text{W}$  range.

**Sensors.** For further miniaturization of the sensors, a closer look at the interior of the temperature sensor ADT7310 is taken. Analog Devices provides the ADT7312, a temperature sensor in die form. It is the same die which is also integrated in the ADT7310 that is used in the hardware setup of this work [19].

It has a thickness of 0.092  $\mu\text{m}$ . As a die has no protective coating, a protective layer needs to be added before it can be integrated into the cell. An appropriate material has to be found as it has to conduct the heat very well and has to be inert in the cell's environment.

Compared to the ADT7310 sensor used in the development setup, a solution with less cables is given by the DS18B20 from Maxim Integrated. This sensor requires only one data and an additional ground line. It communicates with the micro controller through this data line and receives power from the same line. It also has additional features like a CRC-8 generator for calculating a check sum to ensure a reliable communication to the micro controller. Yet the sensor is only available in relatively big packages and thus has to be put into a smaller package for an integration into the cell. The usability in the cell environment is yet to be proven. For a later integration, a minimized custom solution that is optimized for the usage in the cell environment and at cell voltage will provide a suitable solution. **Power supply.** In an ASIC solution, the power supply can either be integrated or completely avoided if the manufacturing process can cope with the available variable battery cell power between 2.7 V and 4.2 V.

#### 5.4. Costs

The prototype presented in this paper with its two Arduino Uno R3 boards, the power bank, some smaller electronic parts and five sensors sums up to a total cost of around 100 USD. With the proposed custom ASIC solution, the costs for the whole system can be reduced to less than 1 USD per chip when mass-produced. Consequently, the described system provides a cost-efficient solution.

## 6. Experimental validation

To research the communication through the pouch cell laminate in detail, the signal before and after the coupling capacitor was measured with a PicoScope 2205 from Pico Technology. One byte was transmitted from the sending Arduino through the pouch cell laminate. For having a highest possible bit change, the binary value 01010101 ( $0 \times 55$ ) was chosen. As the least significant bit is transferred first in the UART communication, a high edge is transmitted directly after the low START bit. At every following bit, the signal level changes until the high STOP bit is achieved after 8 data bits. With the help of these tests, the influence of different coupling capacitor sizes, the type of adhesive for attaching the capacitor plates to the aluminum laminate and the influence of different baud rates, are evaluated. In the following, output signal refers to pin TX from the sending Arduino and input signal to the signal at the pin RX of the receiving Arduino. Thus the output signal is the signal before the coupling capacitor.

For detecting the transferred values, each bit is sampled three times in the middle. However, the signal after the coupling capacitor consists of mainly peaks at the rising edge followed by a fast decline (see Fig. 6) which would make a signal detection in the

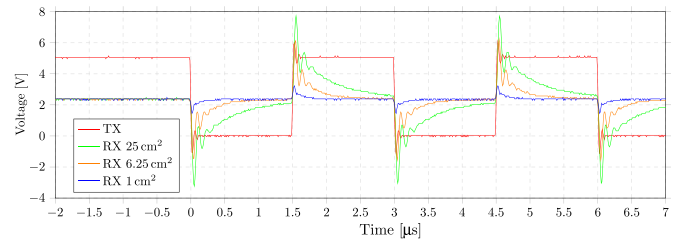


Fig. 6. Influence of different capacitor sizes on the strength of the transmitted signal.

middle impossible. To face this issue, the micro controller has a Schmitt trigger integrated. Since an inverting Schmitt trigger allows a higher input resistance than a non-inverting Schmitt trigger, the former one is used in most applications. At the input of the Schmitt trigger, the signal is pulled to the reference voltage  $V_{add} = 2.5 \text{ V}$  by using a pull up resistor of 1 k $\Omega$ .

The trigger reacts only if the input signal surpasses in the one direction from the defined reference voltage. As an inverting trigger is used, the trigger's output is set to LOW as long as the input signal is above  $V_{add}$ . Once the signal falls below  $V_{add}$ , the trigger changes its state and sets the output signal to HIGH. With this method, the micro controller generates square waves out of the peak signals that are received on the other side of the coupling capacitor. By setting the threshold voltage to a respective value, even very small values can be solidly detected with this approach.

#### 6.1. Influence of capacitor size and adhesive

Different sizes of capacitor plates attached to the aluminum laminate have been investigated. The goal is to use capacitor plates as small as possible to be able to integrate the system in any desired battery cell size. For attaching the capacitor plates to the laminate, both, a thermally conductive adhesive and a normal adhesive have been researched. No difference in the signal quality could be recognized. All used capacitor plates have a quadratic shape with a side length of 1 cm, 2.5 cm and 5 cm. In Fig. 6, the output signals RX from the different capacitors are displayed in comparison to the input signal TX.

It is obvious that a bigger capacitor area leads to a stronger signal with higher peaks. This can however be solved by adjusting the voltage threshold of the Schmitt trigger that is integrated in the receiving micro controller and responsible for identifying the signal.

#### 6.2. Influence of Baud rates

In a further experiment, the influence of different baud rates for the signal transmission has been examined. For the investigation, capacitor plates with a side length of 5 cm have been used. The researched baud rates have been 9600 bd, 750,000 bd and 2,000,000 bd. It has been found that contrary to the transmission of sinusoidal signals as described in [10], the transmission speed does not influence the attenuation of the signal. This effect can be explained with the steep edges of the signal. Changes between HIGH and LOW are performed within a few nanoseconds. The only limitation in this context is the resonance frequency of the setup which should not be undercut. This resonance frequency is limited by the high pass filter that is formed by the coupling capacitor and resistances parallel to it.

## 7. Conclusion

This paper discusses the strong demand for temperature monitoring and particularly in-situ temperature measurements

in Li-Ion battery cells. To overcome the drawbacks of existing analog approaches, a fully digitized system is proposed. By using capacitive coupling, wiring through the cell casing is omitted. Using a digital transmission scheme and corresponding components, reliable and fast data transfers of multiple temperature sensors are provided. In detail, the communication protocol as well as a hardware setup for proof of concept are discussed. In summary, the following requirements for in-situ sensing are satisfied: First, it is shown that the delay between measurements might be reduced to up to 65  $\mu$ s depending on the transmission rate, which is more than sufficient to ensure a safe operation. Second, the potential for high bandwidth with up to 2,000,000 bd enables the integration of multiple sensors in a single cell. Finally, miniaturization options are discussed and further steps towards a fully integrated system are presented, complying to all shape and space requirements and resulting in a cost efficient solution.

Future work will use the developed concept towards an integration of prototype using a Li-Ion pouch cell.

## Acknowledgment

This work was financially supported by the Singapore National Research Foundation under its Campus for Research Excellence And Technological Enterprise (CREATE) program.

## References

- [1] S. Steinhörst, M. Lukaszewicz, S. Narayanaswamy, M. Kauer, S. Chakraborty, Smart cells for embedded battery management, in: Proceedings of the 2nd International Conference on Cyber-Physical Systems, Networks, and Applications (CPSNA 2014), 2014, pp. 59–64, <http://dx.doi.org/10.1109/CPSNA.2014.22>.
- [2] R. Arunachala, S. Arnold, L. Moraleja, T. Pixis, A. Jossen, J. Garche, Influence of cell size on performance of lithium ion battery, in: Presentation at Kraftwerk Batterie, Muenster, Germany, 2015.
- [3] N. Martiny, P. Osswald, C. Huber, A. Jossen, Safety management for electric vehicle batteries in a tropic environment, in: Electric Vehicle Symposium 26, Los Angeles, CA, 2012.
- [4] X. Feng, M. Fang, X. He, M. Ouyang, H. Lu, Languang and Wang, M. Zhang, Thermal runaway features of large format prismatic lithium ion battery using extended volume accelerating rate calorimetry, *J. Power Sources* 255 (2014) 294–301.
- [5] M.S.K. Mutyalu, J. Zhao, J. Li, H. Pan, C. Yuan, X. Li, In-situ temperature measurement in lithium ion battery by transferable flexible thin film thermocouples, *J. Power Sources* 260 (2014) 43–49.
- [6] Z. Li, J. Zhang, B. Wu, J. Huang, Z. Nie, Y. Sun, F. An, N. Wu, Examining temporal and spatial variations of internal temperature in large-format laminated battery with embedded thermocouples, *J. Power Sources* 241 (2013) 536–553.
- [7] C.-Y. Lee, S.-J. Lee, M.-S. Tang, P.-C. Chen, In situ monitoring of temperature inside lithium-ion batteries by flexible micro temperature sensors, *Sensors* 11 (2011) 9942–9950.
- [8] N. Martiny, J. Geder, Y. Wang, W. Kraus, A. Jossen, Development of a thin-film thermocouple matrix for in-situ temperature measurement in a lithium ion pouch cell, in: IEEE SENSORS, IEEE, 2013, <http://dx.doi.org/10.1109/icsens.2013.6688485>.
- [9] N. Martiny, A. Rheinfeld, J. Geder, Y. Wang, A. Jossen, Development of an all Kapton-based thin-film thermocouple matrix for in-situ temperature measurement in a lithium ion pouch cell, *IEEE Sens. J.* (2014), <http://dx.doi.org/10.1109/jsen.2014.2331996>.
- [10] N. Martiny, A. Hornung, M. Schussler, A. Jossen, A capacitively coupled data transmission system for resistance based sensor arrays for in-situ monitoring of lithium-ion battery cells, in: IEEE SENSORS 2014 Proceedings, 2014, <http://dx.doi.org/10.1109/icsens.2014.6985053>.
- [11] P. Balakrishnan, R. Ramesh, T.P. Kumar, Safety mechanisms in lithium-ion batteries, *J. Power Sources* 155 (2006) 401–414.
- [12] T.M. Bandhauer, S. Garimella, T.F. Fuller, A critical review of thermal issues in lithium-ion batteries, *J. Electrochem. Soc.* 158 (3) (2011) R1–R25.
- [13] J.P. Schmidt, S. Arnold, A. Loges, D. Werner, T. Wetzel, E. Ivers-Tiffée, Measurement of the internal cell temperature via impedance: Evaluation and application of a new method, *J. Power Sources* 243 (2013) 110–117, <http://dx.doi.org/10.1016/j.jpowsour.2013.06.013>.
- [14] R. Srinivasan, B.G. Carkhuff, M.H. Butler, A.C. Baisden, Instantaneous measurement of the internal temperature in lithium-ion rechargeable cells, *Electrochim. Acta* 56 (17) (2011) 6198–6204, <http://dx.doi.org/10.1016/j.electacta.2011.03.136>.
- [15] C.-Y. Lee, S.-J. Lee, Y.-M. Lee, M.-S. Tang, P.-C. Chen, Y.-M. Chang, In situ monitoring of temperature using flexible micro temperature sensors inside polymer lithium-ion battery, in: 7th IEEE International Conference on Nano/Micro Engineered and Molecular Systems (NEMS), IEEE, 2012, <http://dx.doi.org/10.1109/nems.2012.6196871>.
- [16] A. Otto, S. Rzepka, T. Mager, B. Michel, C. Lanciotti, T. Günther, O. Kanoun, Battery management network for fully electrical vehicles featuring smart systems at cell and pack level, in: G. Meyer (Ed.), *Advanced Microsystems for Automotive Applications*, Springer, Berlin, Heidelberg, 2012, [http://dx.doi.org/10.1007/978-3-642-29673-4\\_1](http://dx.doi.org/10.1007/978-3-642-29673-4_1).
- [17] V. Lorentz, M. Wenger, J. Grosch, M. Giegerich, M. Jank, M. Marz, L. Frey, Novel cost-efficient contactless distributed monitoring concept for smart battery cells, in: IEEE International Symposium on Industrial Electronics (ISIE), 2012, 1342–1347, <http://dx.doi.org/10.1109/ISIE.2012.6237285>.
- [18] Analog Devices, Inc., ADT7310 datasheet: 16-Bit Digital SPI Temperature Sensor, 2011.
- [19] Analog Devices, Inc., ADT7312 Datasheet: Automotive,  $\pm 1^\circ\text{C}$  Accurate, 16-Bit,  $175^\circ\text{C}$ , Digital SPI Temperature Sensor in Die Form, 2012.

## Glossary

*Li-Ion*: Lithium Ion  
*SoS*: State-of-Safety  
*HF*: Hydrofluoric Acid  
*IC*: Integrated Circuit  
*CRC*: Cyclic Redundancy Check  
*UART*: Universal Asynchronous Receiver/Transmitter  
*SPI*: Serial Peripheral Interface  
*USB*: Universal Serial Bus  
*SoC*: System-on-Chip  
*ASIC*: Application-Specific Integrated Circuit  
*DFN*: Dual-Flat No-leads  
*BMS*: Battery Management System